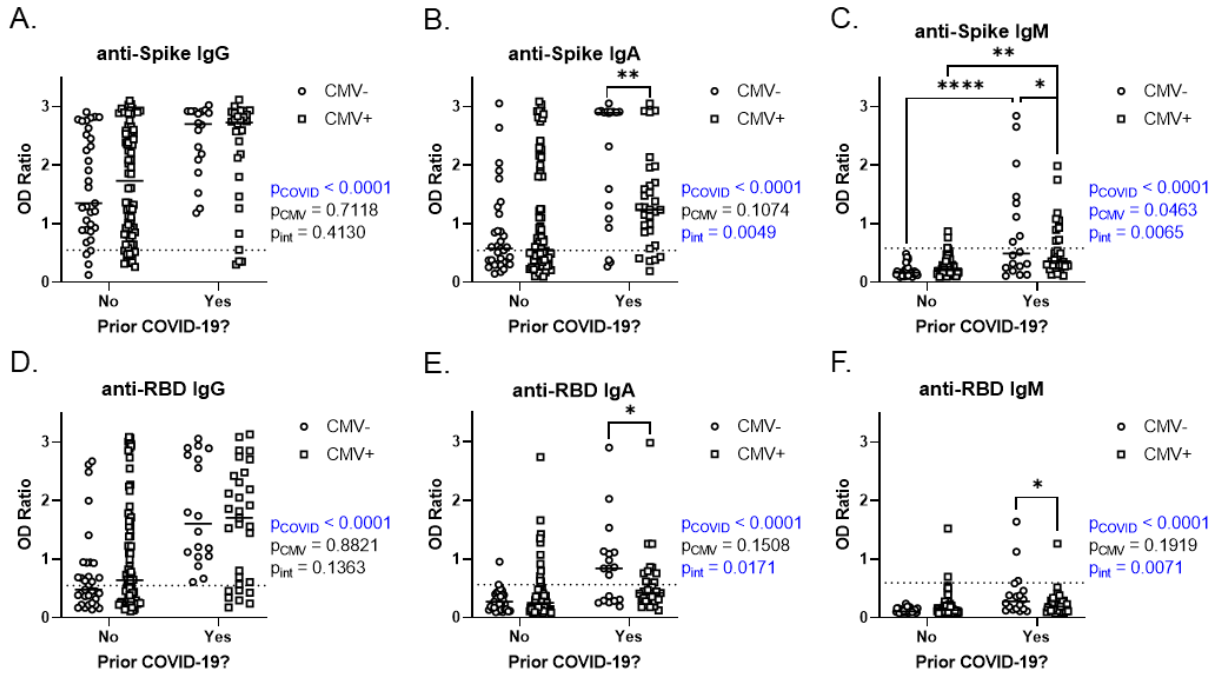


790

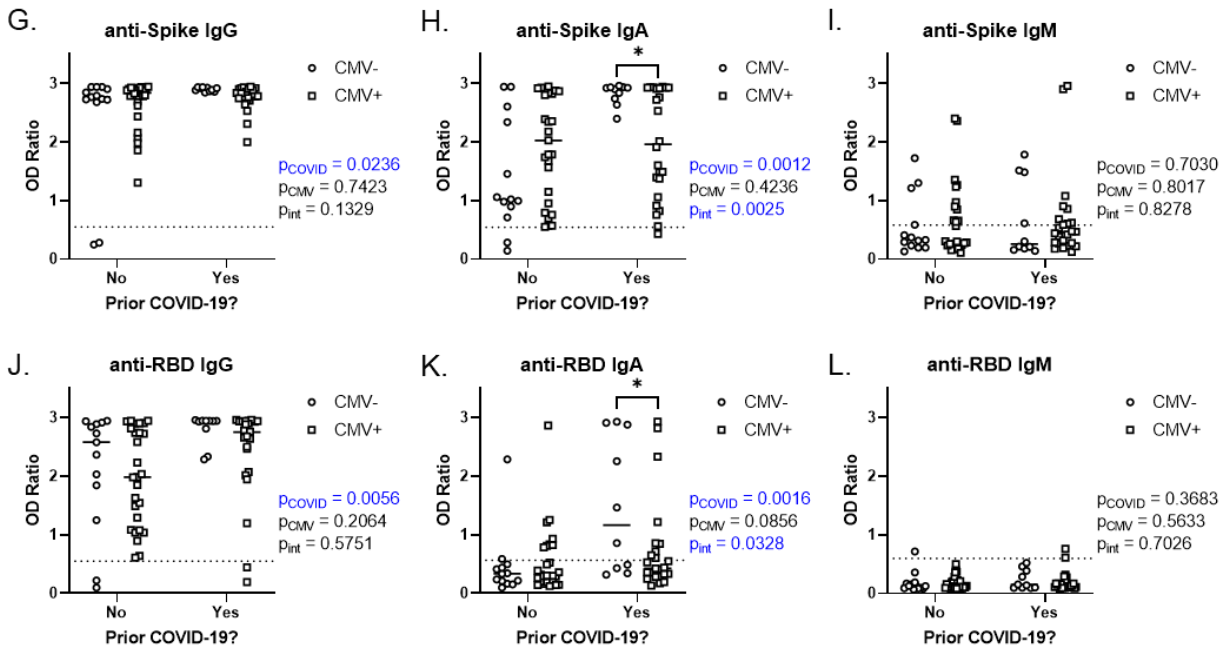
791 **Supplementary Figure 1. Intra-individual comparisons of antibody levels and**
 792 **neutralization capacity after 2 and 3 COVID-19 vaccine doses in older adults.**

793 Matched intra-individual data post-dose 2 (PD2) and post-dose 3 (PD3) measurements of serum
 794 anti-Spike IgG (A), IgA (B) and IgM (C) antibodies, as well as anti-receptor binding domain
 795 (RBD) IgG (D), IgA (E), and IgM (F) antibodies. Matched intra-individual antibody
 796 neutralization capacity between 2 and 3 vaccine doses against wildtype (G) and beta variant (H)
 797 SARS-CoV-2. Dotted lines indicate the threshold of detection. Each data point indicates an
 798 individual participant and lines connect data from a single participant across post-dose 2 and
 799 post-dose 3 time points. Intra-individual associations between CMV serostatus and vaccine dose
 800 were assessed by paired two-way ANOVA, with Šidák's test post-hoc analysis. * $p < 0.05$,
 801 ** $p < 0.01$, *** $p < 0.001$.

Post-Dose 2

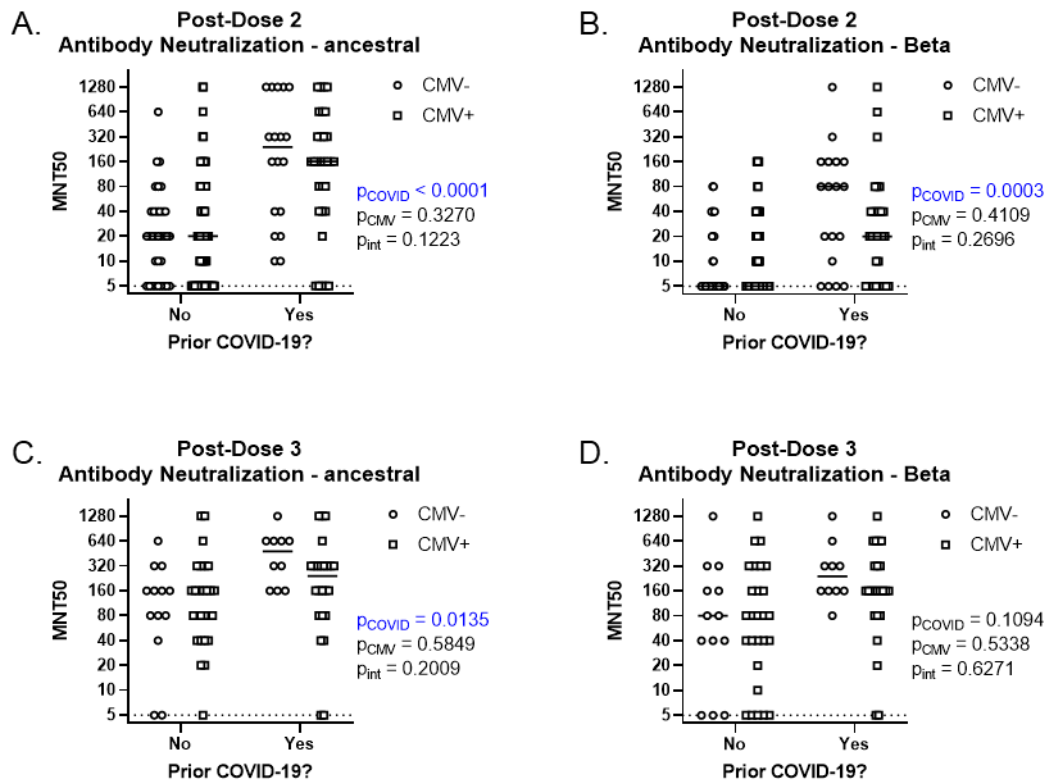


Post-Dose 3

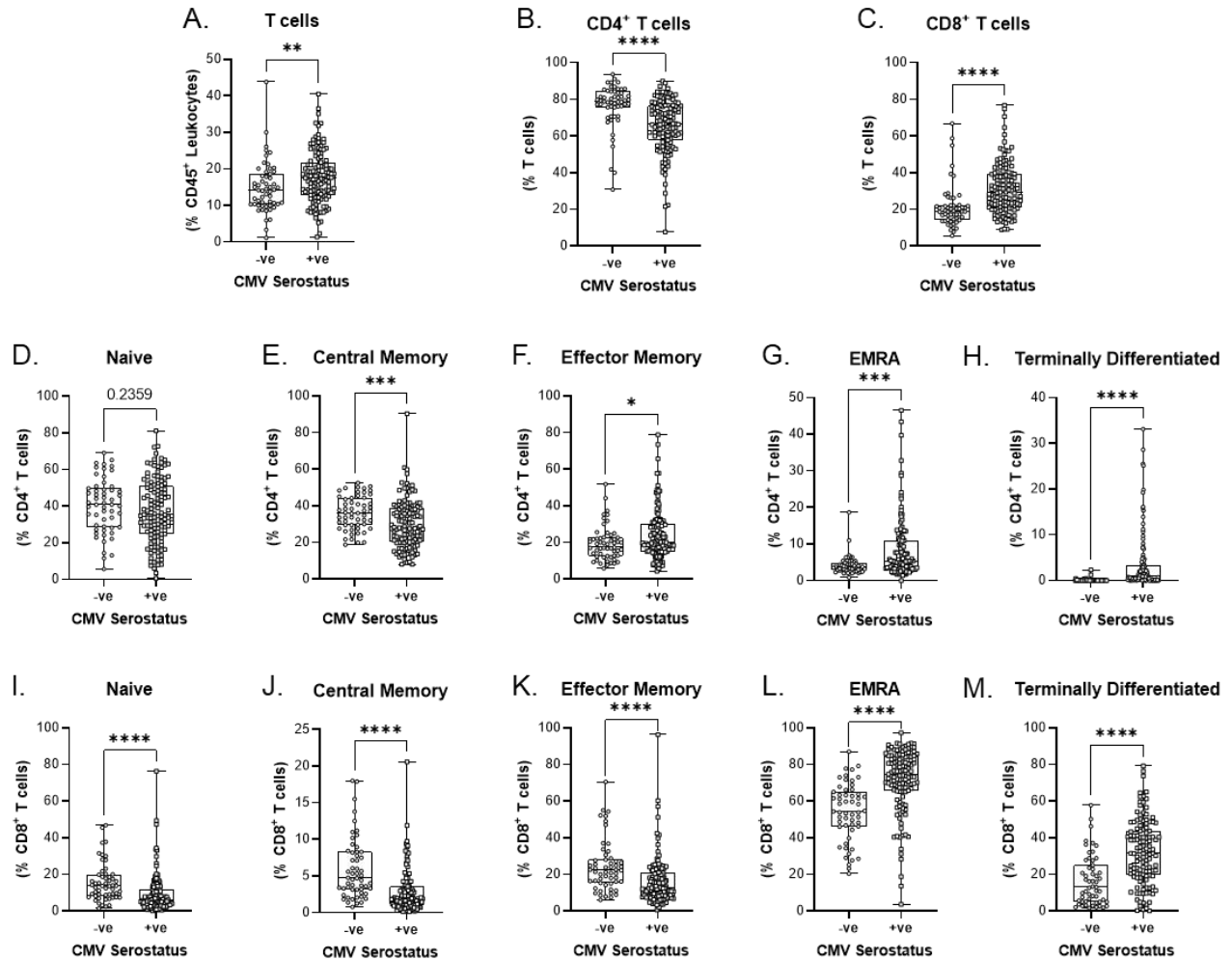


802
 803 **Supplementary Figure 2. Antibodies by CMV serostatus and prior SARS-CoV-2 infection after two**
 804 **and three COVID-19 vaccines in older adults.**

805 SARS-CoV-2 anti-Spike and anti-RBD antibodies were measured in serum by ELISA. Post-dose 2: anti-
 806 Spike IgG (A), IgA (B) and IgM (C) antibodies, and anti-receptor binding domain (RBD) IgG (D), IgA
 807 (E), and IgM (F) antibodies. Post-dose 3: anti-Spike IgG (G), IgA (H) and IgM (I) antibodies, and anti-
 808 receptor binding domain (RBD) IgG (J), IgA (K), and IgM (L) antibodies. Dotted lines indicate the
 809 threshold of detection. Each data point indicates an individual participant, and the center line indicates the
 810 median. Associations between CMV serostatus and prior COVID-19 were assessed by two-way ANOVA,
 811 with Tukey's test post-hoc analysis. * $p < 0.05$, ** $p < 0.01$.



812
 813 **Supplementary Figure 3. Antibody neutralization capacity by CMV serostatus and prior**
 814 **SARS-CoV-2 infection after two and three COVID-19 vaccines in older adults.**
 815 Serum antibody neutralization capacity was assessed by MNT50 with live SARS-CoV-2 virus.
 816 Post-dose 2: wildtype (A) and beta variant (B) SARS-CoV-2 neutralization. Post-dose 3:
 817 wildtype (C) and beta variant (D) SARS-CoV-2 neutralization. Dotted lines indicate the
 818 threshold of detection. Each data point indicates an individual participant, and the center line
 819 indicates the median. Associations between CMV serostatus and vaccine dose were assessed by
 820 two-way ANOVA, with Tukey's test post-hoc analysis.



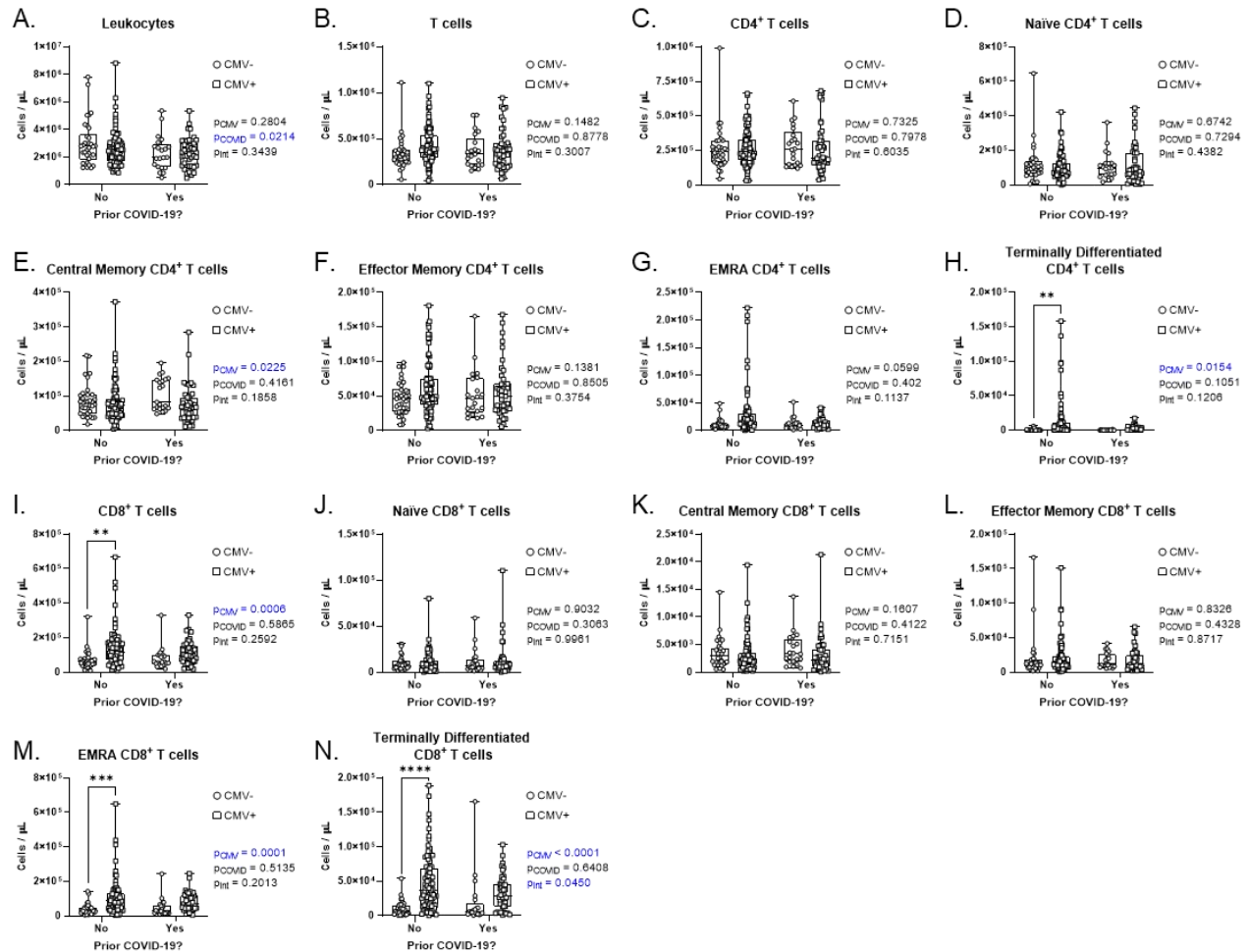
821

822 **Supplementary Figure 4. Effect of CMV serostatus on the circulating T cell repertoire in**
 823 **older adults.**

824 T cell populations in whole blood were assessed by flow cytometry. (A) Prevalence of T cells as
 825 a proportion of total leukocytes. Prevalence of (B) CD4⁺ T cells and (C) CD8⁺ T cells as a
 826 proportion of total T cells. CD4⁺ T cell subsets as a proportion of total CD4⁺ T cells: (D) naïve;
 827 (E) central memory; (F) effector memory; (G) EMRA; (H) terminally differentiated. CD8⁺ T cell
 828 subsets as a proportion of total CD4⁺ T cells: (I) naïve; (J) central memory; (K) effector memory;
 829 (L) EMRA; (M) terminally differentiated. Each data point indicates an individual participant.

830 Data are presented as box and whisker plots, minimum to maximum, where the center line
 831 indicates the median. Associations between T cell subsets and CMV serostatus were assessed by
 832 Student's *t* test with Welch's correction or Mann-Whitney *U* test, according to normality.

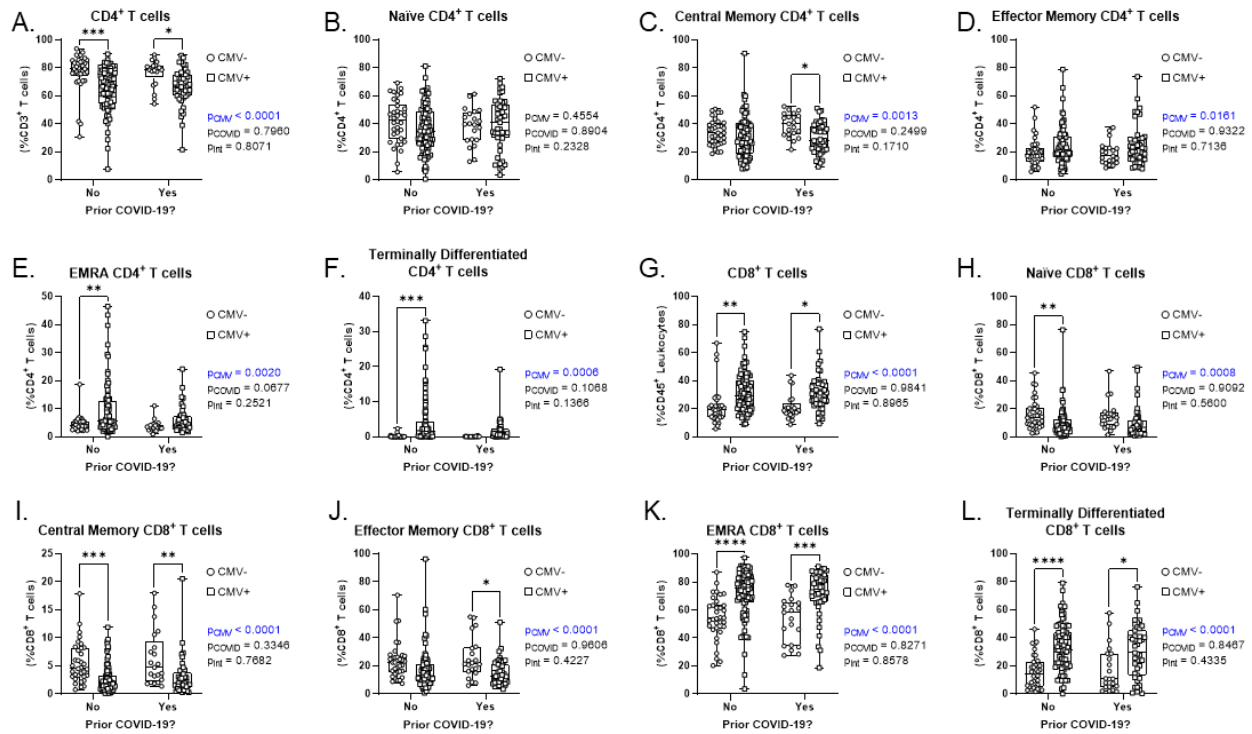
833 **p*<0.05, ***p*<0.01, ****p*<0.001, *****p*<0.0001.



834

835 **Supplementary Figure 5. Effects of CMV serostatus and prior COVID-19 on the**
 836 **circulating T cell repertoire in older adults – cell counts.**

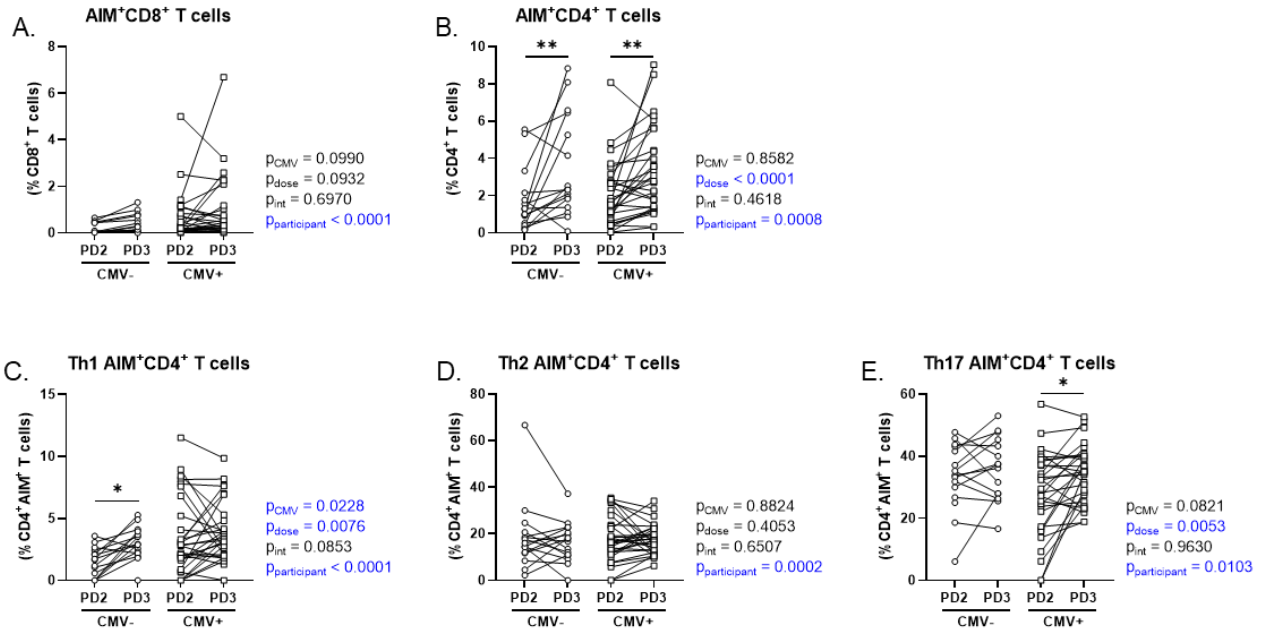
837 T cell populations in whole blood were assessed by flow cytometry. Absolute cell counts of: (A)
 838 total leukocytes; (B) total T cells; (C) total CD4⁺ T cells. Absolute cell counts of CD4⁺ T cells:
 839 (D) naïve; (E) central memory; (F) effector memory; (G) EMRA; (H) terminally differentiated.
 840 Absolute cell counts of CD8⁺ T cells: (I) total; (J) naïve; (K) central memory; (L) effector
 841 memory; (M) EMRA; (N) terminally differentiated. Each data point indicates an individual
 842 participant. Data are presented as box and whisker plots, minimum to maximum, where the
 843 center line indicates the median. Associations between CMV serostatus and prior COVID-19
 844 were assessed by two-way ANOVA, with Tukey's test post-hoc analysis. *** $p < 0.001$,
 845 ** $p < 0.0001$.



846

847 **Supplementary Figure 6. Effect of CMV serostatus and prior COVID-19 on the circulating**
 848 **T cell repertoire in older adults – frequency.**

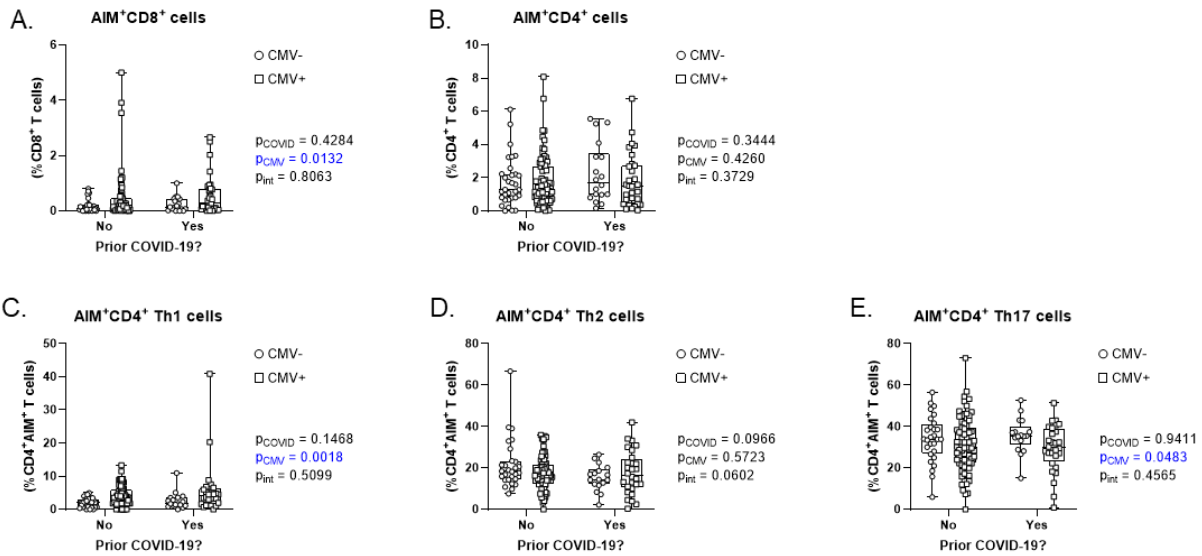
849 T cell populations in whole blood were assessed by flow cytometry. (A) Prevalence of CD4⁺ T
 850 cells as a proportion of total T cells. CD4⁺ T cell subsets as a proportion of total CD4⁺ T cells:
 851 (B) naïve; (C) central memory; (D) effector memory; (E) EMRA; (F) terminally differentiated.
 852 CD8⁺ T cell subsets as a proportion of total CD8⁺ T cells: (G) naïve; (H) central memory; (I)
 853 effector memory; (J) EMRA; (K) terminally differentiated. Associations between T cell subsets
 854 and CMV serostatus were assessed by Student's t test with Welch's correction or Mann-Whitney
 855 U test, according to normality. Absolute cell counts of: (A) total leukocytes; (B) total T cells; (C)
 856 total CD4⁺ T cells. Absolute cell counts of CD4⁺ T cells: (D) naïve; (E) central memory; (F)
 857 effector memory; (G) EMRA; (H) terminally differentiated. Absolute cell counts of CD8⁺ T
 858 cells: (I) total; (J) naïve; (K) central memory; (L) effector memory; (M) EMRA; (N) terminally
 859 differentiated. Each data point indicates an individual participant. Data are presented as box and
 860 whisker plots, minimum to maximum, where the center line indicates the median. Associations
 861 between CMV serostatus and prior COVID-19 were assessed by two-way ANOVA, with
 862 Tukey's test post-hoc analysis. * $p < 0.05$, ** $p < 0.01$, *** $p < 0.001$, **** $p < 0.0001$.



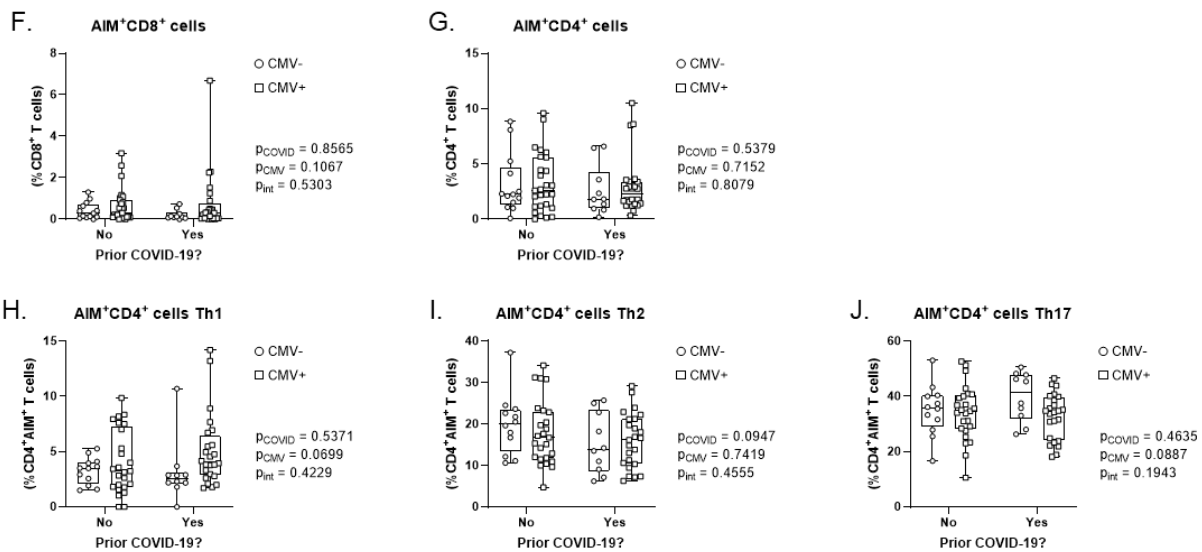
863
 864 **Supplementary Figure 7. Intra-individual comparisons of CD4⁺ and CD8⁺ T cell activation**
 865 **induced memory responses to SARS-CoV-2 Spike peptide pools in older adults by CMV**
 866 **serostatus.**

867 T cell memory responses to SARS-CoV-2 Spike protein were assessed by activation induced
 868 marker assay. (A) Spike SARs-CoV-2-specific AIM⁺CD8⁺ T cells (expressing CD69 and
 869 CD137) as a proportion of total CD8⁺ T cells. (B) Spike SARs-CoV-2-specific AIM⁺CD4⁺ T
 870 cells (expressing CD25 and OX40L) as a proportion of total CD4⁺ T cells. Spike SARs-CoV-2-
 871 specific AIM⁺CD4⁺ T cell functional Th1 (C), Th2 (D), and Th17 (E) subsets. Each data point
 872 indicates an individual participant and lines connect data from a single participant across post-
 873 dose 2 and post-dose 3 time points. Intra-individual associations between CMV serostatus and
 874 vaccine dose were assessed by paired two-way ANOVA, with Šidák's test post-hoc analysis.
 875 * $p < 0.05$, ** $p < 0.01$.

Post-Dose 2

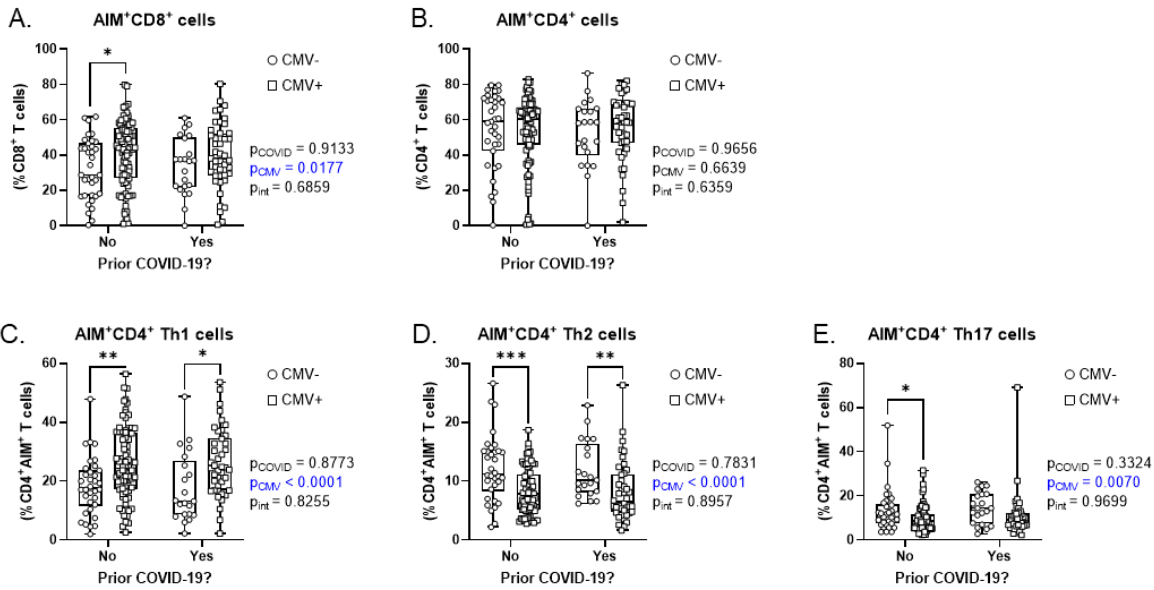


Post-Dose 3

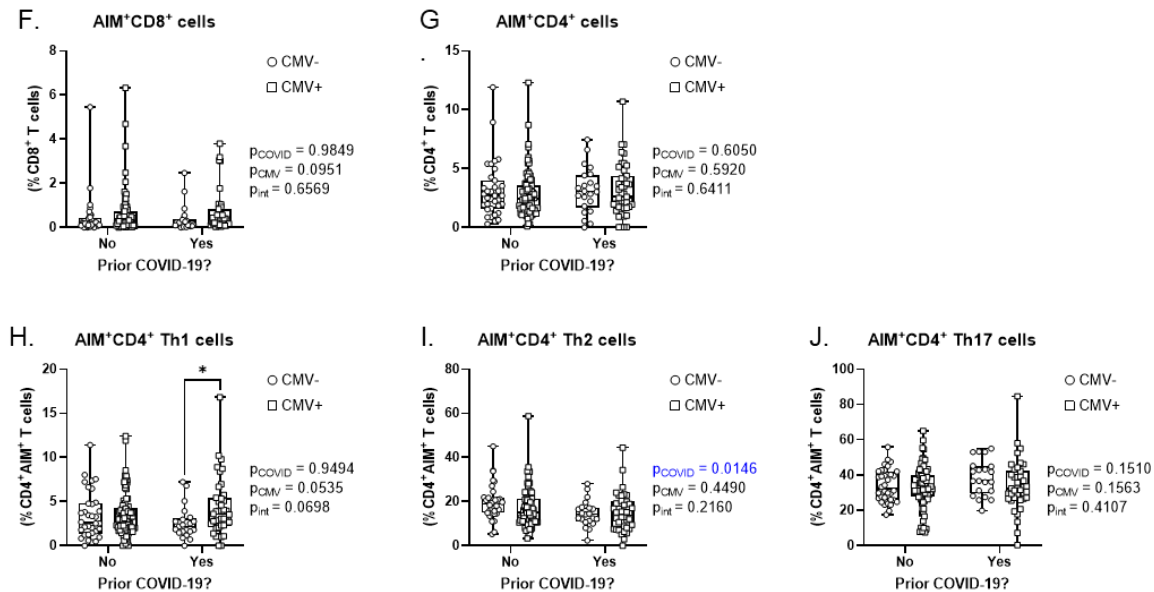


876
 877 **Supplementary Figure 8. CD4⁺ and CD8⁺ T cell activation induced memory responses to**
 878 **SARS-CoV-2 Spike peptide pools after COVID-19 in older adults by CMV serostatus.**
 879 Post-dose 2: (A) Spike SARS-CoV-2-specific AIM⁺CD8⁺ T cells (expressing CD69 and CD137)
 880 were measured as a proportion of total CD8⁺ T cells. (B) Spike SARS-CoV-2-specific
 881 AIM⁺CD4⁺ T cells (expressing CD25 and OX40L) were measured as a proportion of total
 882 CD4⁺ T cells. Spike SARS-CoV-2-specific AIM⁺CD4⁺ T cell functional Th1 (C), Th2 (D), and
 883 Th17 (E) subsets. Post-dose 3: (F) Spike SARS-CoV-2-specific AIM⁺CD8⁺ T cells as a
 884 proportion of total CD8⁺ T cells. (G) Spike SARS-CoV-2-specific AIM⁺CD4⁺ T cells as a
 885 proportion of total CD4⁺ T cells. Spike SARS-CoV-2-specific AIM⁺CD4⁺ T cell functional Th1
 886 (H), Th2 (I), and Th17 (J) subsets. Each data point indicates an individual participant. Data are
 887 presented as box and whisker plots, minimum to maximum, where the center line indicates the
 888 median. Associations between CMV serostatus and prior COVID-19 were assessed by two-way
 889 ANOVA, with Tukey’s test post-hoc analysis. **p*<0.05.

CytoStim



Influenza HA



890
891
892
893
894
895
896
897
898
899
900
901

Supplementary Figure 9. CD4⁺ and CD8⁺ T cell activation induced memory responses to CytoStim and influenza HA peptide pools after COVID-19 in older adults by CMV serostatus.

CytoStim-induced responses: (A) AIM⁺CD8⁺ T cells (expressing CD69 and CD137) as a proportion of total CD8⁺ T cells; (B) AIM⁺CD4⁺ T cells (expressing CD25 and OX40L) as a proportion of total CD4⁺ T cells; AIM⁺CD4⁺ T cell functional Th1 (C), Th2 (D), and Th17 (E) subsets. Influenza HA-induced responses: (F) AIM⁺CD8⁺ T cells (expressing CD69 and CD137) as a proportion of total CD8⁺ T cells; (G) AIM⁺CD4⁺ T cells (expressing CD25 and OX40L) as a proportion of total CD4⁺ T cells; AIM⁺CD4⁺ T cell functional Th1 (H), Th2 (I), and Th17 (J) subsets. Each data point indicates an individual participant. Data are presented as box and whisker plots, minimum to maximum, where the center line indicates the median. Associations between CMV serostatus and prior COVID-19 were assessed by two-way ANOVA, with Tukey's test post-hoc analysis. **p*<0.05, ***p*<0.01, ****p*<0.001.